Inorganica Chimica Acta 439 (2016) 49–54

Contents lists available at ScienceDirect

Inorganica Chimica Acta

journal homepage: www.elsevier.com/locate/ica

Synthesis, hydrogen-bonded 1D structure, and abrupt spin transition between high-spin (HS) and an ordered [HS–HS–HS–LS] of a mononuclear iron(III) complex $[Fe^{III}(Him)_2(4\text{-MeOhapen})]CF_3SO_3$ (Him = imidazole, 4-MeOhapen = *N*,*N*′-bis-(2-oxy-4-methoxyacetophenylidene)ethylenediamine)

Kyohei Miyano [a], Takahiro Nishida [a], Hiromasa Ono [a], Daisuke Hamada [a], Takeshi Fujinami [a], Naohide Matsumoto [a,*], Yukinari Sunatsuki [b]

[a] Department of Chemistry, Faculty of Science, Kumamoto University, Kurokami 2-39-1, Kumamoto 860-8555, Japan
[b] Department of Chemistry, Faculty of Science, Okayama University, Tsushima-naka 1-1, Okayama 700-8530, Japan

ARTICLE INFO

Article history:
Received 19 June 2015
Received in revised form 3 September 2015
Accepted 24 September 2015
Available online 9 October 2015

Keywords:
Iron(III)
Spin crossover
Imidazole
N_2O_2 Schiff-base ligand
Hydrogen bonds
1D structure

ABSTRACT

A SCO iron(III) complex $[Fe^{III}(Him)_2(4MeOhapen)]CF_3SO_3$ was synthesized, where Him = imidazole and 4-MeOhapen = *N*,*N*′-bis(2-oxy-4-methoxyacetophenylidene)ethylenediamine. Fe^{III} ion has an octahedral coordination geometry with N_2O_2 donor atoms of the equatorial tetradentate ligand (4-MeOhapen) and two nitrogen atoms of two imidazoles (Him) at the axial positions. The adjacent cations are bridged by $CF_3SO_3^-$ ion through NH···O hydrogen bonds between Him and $CF_3SO_3^-$ to give a one-dimensional chain structure $\{[Fe^{III}(Him)_2(4MeO\text{-}hapen)]CF_3SO_3\}_{1\infty}$. The magnetic susceptibility measurements showed that complex exhibits an abrupt spin transition between a single HS phase and a symmetry-breaking [HS–HS–HS–LS] phase and another transition around 80 K. The single-crystal X-ray analyses at 296 and 150 K revealed the structures at a single HS and [HS–HS–HS–LS] states.

1. Introduction

Spin crossover (SCO) phenomenon is an inter-conversion between high-spin (HS) and low-spin (LS) states by external perturbations, such as temperature, pressure, and light irradiation [1]. Among the SCO complexes reported so far, Fe^{II} and Fe^{III} complexes have been the most intensively studied [1]. It is well known that Fe sites in some heme proteins exhibit SCO behavior [2] and as their model compounds iron porphyrin and macrocyclic complexes have been extensively studied [3]. As a simple model compound for some heme proteins, Nishida in 1975 first synthesized a family of Fe^{III} complexes $[Fe^{III}B_2L]BPh_4$ with salen-type N_2O_2 ligand L and two axial monodentate ligand B, and counter anion BPh_4^- (BPh_4^- = tetraphenylborate) [4]. Later, Matsumoto, Murray, and Real synthesized SCO Fe^{III} complexes $[Fe^{III}B'_2L']Y$ with analogous Schiff-base ligands L′, monodentate ligand B′, and various counter anion Y′ [5–7]. These studies demonstrated that (1) A favorable conformation of the planar ligand L' can induce SCO property and especially "hapen-type" ligand gives a favorable conformation which makes a large torsion of O–Fe–O angle during the spin transition from HS to LS state due to the steric repulsion between en (ethylenediamine moiety) and methyl group of *o*-hydroxyacetophenone moieties (hapen = *N*,*N*′-bis(2-oxyacetophenylidene)-ethylenediamine) [8]. (2) Intermolecular hydrogen bond via axial imidazole group gives a positive effect to induce abrupt spin transition [9]. (3) The steric requirements from methoxy group of hapen ligand and counter anion modify the assembly structure to influence the SCO property [8,9].

A family of the complexes $[Fe^{III}(Him)_2(hapen)]Y$ would give interesting SCO properties with hysteresis and multi-step. In this study, we synthesized a Fe^{III} complex $[Fe^{III}(Him)_2(4\text{-MeOhapen})]CF_3SO_3$, where 4-MeOhapen denotes *N*,*N*′-bis(2-oxy-4-methoxyacetophenylidene)ethylenediamine). The complex has a hydrogen-bonded 1D structure bridged by $CF_3SO_3^-$ anion, and shows a spin transition between HS and ordered [HS–HS–HS–LS] phases. Such symmetry breaking-phase transition attract much attention [10]. We report here the synthesis, SCO property, and crystal structures at HS and [HS–HS–HS–LS] states (Scheme 1).

* Corresponding author. Tel./fax: +81 96 342 3390.
E-mail address: naohide@aster.sci.kumamoto-u.ac.jp (N. Matsumoto).

http://dx.doi.org/10.1016/j.ica.2015.09.031
0020-1693/

2. Experimental

2.1. General

All reagents and solvents used in this study are commercially available from Tokyo Kasei Co., Ltd., Tokyo, Japan and Wako Pure Chemical Industries, Ltd., Osaka, Japan, and were used without further purification. All of the synthetic procedures were performed in air.

2.2. Preparation of materials

2.2.1. Preparations of H_2(4-MeOhapen) and precursor iron(III) complex [Fe^{III}Cl(4-MeOhapen)]·H_2O

The ligand, *N*,*N*′-bis(4-methoxy-2-hydroxyacetophenylidene) ethylenediamine, abbreviated as H_2(4-MeOhapen), was prepared according to the general synthetic procedure of salen-type Schiff-base ligand [8]. To a solution of 4-methoxy-2-hydroxyacetophenone (0.1 mol, 16.62 g) in 50 mL of methanol was added a solution of ethylenediamine (0.05 mol, 3.01 g) in 50 mL of methanol, and the mixture was stirred for 30 min on a hot-plate and cooled to room temperature. Yellow crystals precipitated were collected by suction filtration, washed with a small amount of methanol and diethyl ether, and dried in vacuo. Precursor iron(III) complex [Fe^{III}Cl(4-MeOhapen)]·H_2O was prepared by the reaction of H_2(4-MeOhapen) (17.8 g, 0.05 mol), $FeCl_3$ (8.1 g, 0.05 mol), and trimethylamine (10.1 g, 0.1 mmol) with 1:1:2 in methanol according to the method applied for [Fe^{III}Clsalen] [5b]. Black precipitates were collected by suction filtration and washed with diethyl ether. Yield: 20.3 g (92%).

2.2.2. Preparation of iron(III) complex [Fe^{III}(Him)$_2$(4-MeOhapen)]CF_3SO_3

To a suspension of [Fe^{III}Cl(4-MeOhapen)]·H_2O (1 mmol, 0.44 g) in 30 mL of methanol was added an excess of imidazole (10 mmol, 0.68 g), and the mixture was stirred for 10 min on a hot-plate and then filtered. To the filtrate was added a solution of $NaCF_3SO_3$ (1 mmol, 0.17 g) in 5 mL of methanol. The resulting solution was allowed to stand for a few days, during which time black plate-like crystals precipitated, and they were collected by suction filtration, washed with small amount of diethyl ether, and dried in air. Black plate crystals were obtained. Yield: 0.172 g (25%). *Anal.* Calc. for [Fe^{III}(Him)$_2$(4-MeOhapen)]CF_3SO_3 ($C_{26}H_{30}N_6O_4FeCF_3SO_3$): C, 46.63; H, 4.35; N, 12.08. Found: C, 46.83; H, 4.34; N, 12.09%.

2.3. Physical measurements

Elemental analyses (C, H, and N) were carried out at the Center for Instrumental Analysis of Kumamoto University. Thermogravimetric analysis (TGA) was measured on a TG/DTA6200 (Seiko Instrument Inc.). The sample of ca. 2 mg was heated from room temperature to 120 °C in the heating mode at 2 °C min^{-1}, kept at 120 °C for 60 min and then cooled from 120 °C to room temperature. Magnetic susceptibilities were measured by a Quantum Design MPMS-XL5 magnetometer in the temperature range of 5–300 K at the 2 K min^{-1} under an applied magnetic field of 0.5 T. The calibration was performed with palladium metal. Corrections for diamagnetism were applied using Pascal's constants [11].

2.4. Crystallographic data collection and structure analyses

X-ray diffraction data were collected using a Rigaku RAXIS RAPID imaging plate diffractometer using graphite monochromated Mo Kα radiation (λ = 0.71073 Å). The temperature of the crystal was maintained at the selected value by means of a Rigaku cooling device within an accuracy of ±2 K. The X-ray diffraction data were collected at 296, and 150 K. After the data collection at 296 K, the crystal was cooled from 296 to 200 K with the cooling rate of 3 K min^{-1}, and then the crystal was cooled slowly from 200 to 150 K at the rate of 0.1 K min^{-1}. The crystal was kept at 150 K for one day, and the data collection was started. The X-ray diffraction data collected after quick cooling showed a poor quality to determine the crystal structure. The data were corrected for Lorentz, polarization and absorption effects. The structures were solved by a direct method, and expanded using the Fourier technique. Hydrogen atoms were fixed at the calculated positions and refined using a riding model. All calculations were performed using the CrystalStructure crystallographic software package [12].

3. Results and discussion

3.1. Synthesis and characterization of iron(III) complex [Fe^{III}(Him)$_2$(4-MeOhapen)]CF_3SO_3

The Fe^{III} complex [Fe^{III}(Him)$_2$(4-MeOhapen)]CF_3SO_3 was prepared according to the synthetic procedure applied for the synthesis of [Fe^{III}(Him)$_2$(4-MeOhapen)]PF_6 [8b]. The precursor Fe^{III} complex [Fe^{III}Cl(4-MeOhapen)]·H_2O was obtained by mixing the ligand H_2(4-MeOhapen), iron(III) chloride anhydrate, and triethylamine in a 1:1:2 M ratio in methanol. The Fe^{III} complex [Fe^{III}(Him)$_2$(4-MeOhapen)]CF_3SO_3 was obtained as well grown black plate-like crystals by mixing [Fe^{III}Cl(4-MeOhapen)]·H_2O, imidazole, and $NaCF_3SO_3$ in a 1:10:1 M ratio in methanol. The C, H, and N elemental analyses agreed with the formula [Fe^{III}(Him)$_2$(4-MeOhapen)]CF_3SO_3. The thermogravimetric analysis (TGA) detected no crystal solvent. Thermochromic behaviors in the solution and solid states are shown in Fig. 1. The ethanol solution of the compound showed a visible thermochromism from orange red at room temperature to dark green–blue at liquid nitrogen temperature. Red and green–blue colors are typical colors for HS and LS states with this type of Fe^{III} complexes, respectively. In the solid state, brown color of the ground sample at room temperature changed to a black brown at liquid-nitrogen temperature, suggesting an incomplete SCO in the solid state.

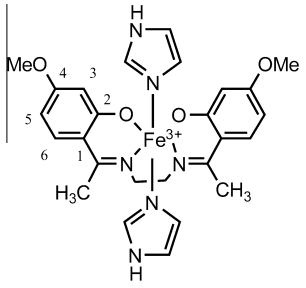

Scheme 1. Structure of [Fe^{III}(Him)$_2$(4-MeOhapen)]$^+$.

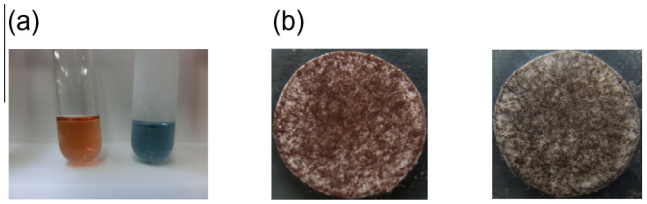

Fig. 1. (a) Thermochromism of [Fe^{III}(Him)$_2$(4-MeOhapen)]CF_3SO_3 at room (left) and liquid nitrogen (right) temperatures in the diluted ethanol solutions. (b) Thermochromism of the ground sample at room (left) and liquid nitrogen (right) temperatures in the solid state.

3.2. Temperature-dependence of magnetic properties

The magnetic susceptibility (χ_M) of the polycrystalline sample was measured in the temperature range 5–300 K under an applied magnetic field of 0.5 T at a sweep rate of 2 K min^{-1}. The magnetic susceptibility was measured while lowering the temperature from 300 to 5 K in the first run. Subsequently, the magnetic susceptibility was measured while raising the temperature from 5 to 300 K in the second run. The $\chi_M T$ vs. T plots are shown in Fig. 2, in which the $\chi_M T$ vs. T plots for the cooling and warming modes are drawn as blue and red colors, respectively. The experimental $\chi_M T$ vs. T profile can be examined in terms of the spin-only values of the HS ($S = 5/2$) and LS ($S = 1/2$) states of Fe^{III} ions with the $3d^5$ electronic configuration; the theoretical spin-only $\chi_M T$ values for the HS ($S = 5/2$) and LS ($S = 1/2$) states are 4.37 and 0.375 cm^3 mol^{-1} K, respectively.

On lowering the temperature from 300 K, the $\chi_M T$ value has a constant value of ca. 4.64 cm^3 mol^{-1} K above 200 K and then decreases abruptly at around 190 K to reach a plateau region of ca. 3.5 cm^3 mol^{-1} K below 180 K. The $\chi_M T$ value of ca. 4.64 cm^3 mol^{-1} K above 200 K is compatible with 4.37 cm^3 mol^{-1} K of the spin-only HS value. The $\chi_M T$ value of ca. 3.5 cm^3 mol^{-1} K at the plateau region below 180 K is comparable to the estimated value of 3.37 cm^3 mol^{-1} K corresponding to 3/4 HS ($S = 5/2$) and 1/4 LS ($S = 1/2$) species, i.e. [HS–HS–HS–LS] phase. The spin-transition temperature $T_{1/2}$ assigned between 4HS and HS–HS–HS–LS states is evaluated to be $T_{1/2\uparrow} = 193$ K and $T_{1/2\downarrow} = 192$ K, respectively. Though it looks that the compound has a small hysteresis at the fast scan rate of 2 K min^{-1}, the scan rate dependence can give the more detailed mechanism of the spin transition as observed in the literatures [13].

On decreasing the temperature further at the scan speed of 2 K min^{-1}, the $\chi_M T$ vs. T plots show a shoulder at ca. 80 K, suggesting a spin transition from HS–HS–HS–LS phase to an unidentified phase. In the warming mode, the $\chi_M T$ vs. T plots show a shallow minimum around ca. 80 K and the profile is not accord with that in the cooling mode. This behavior around 80 K is just a kinetic effect that depends on the scan rate. The dip in the χT curve recorded in the warming mode is caused by the release of the kinetic arrest, as observed in $\{[Zn_{1-x}Fex(bbtr)_3](ClO_4)_2\}_\infty$ ($x = 0.02$–1, bbtr = 1,4-di(1,2,3-triazol-1-yl)-butane) [14].

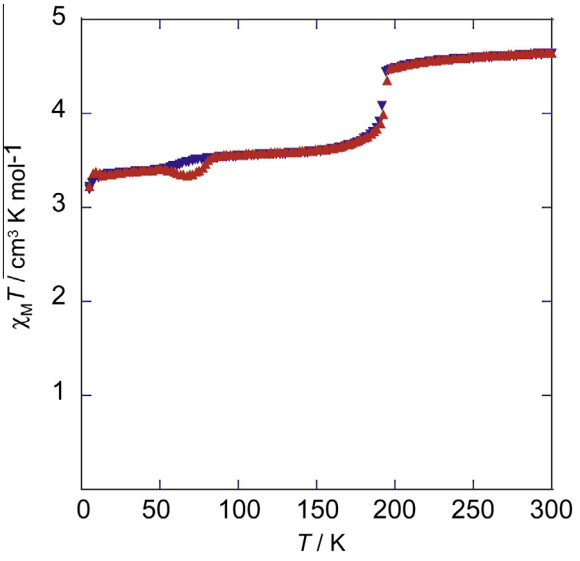

Fig. 2. $\chi_M T$ vs. T plots of $[Fe^{III}(Him)_2(4\text{-MeOhapen})]CF_3SO_3$, in which the data in the cooling and warming modes are drawn as blue and red colors, respectively. (For interpretation of the references to color in this figure legend, the reader is referred to the web version of this article.)

3.3. Crystal structure

The X-ray diffraction analyses were measured at 296 and 150 K. The crystallographic data are listed in Table 1. Relevant coordination bond distances and angles, and hydrogen-bond distances are given in Table 2. At 296 K, compound crystallized in a monoclinic space group $C2/c$ (No. 15) with $Z = 8$, and the unique crystallographic unit consists of one $[Fe^{III}(Him)_2(4\text{-MeOhapen})]^+$ and one $CF_3SO_4^-$ anion. At 150 K compound crystallized in a triclinic space group $P\bar{1}$ (No. 2) with $Z = 8$, and the unique crystallographic unit consists of four cations $[Fe^{III}(Him)_2(4\text{-MeOhapen})]^+$ and four $CF_3SO_4^-$ anions. It demonstrates that the crystal system and space group change from monoclinic $C2/c$ at 296 K to $P\bar{1}$ at 150 K.

3.3.1. Structure at 296 K

The molecular structure of the $[Fe^{III}(Him)_2(4\text{-MeOhapen})]^+$ part with the atom numbering scheme at 296 K is shown in Fig. 3. The Fe^{III} ion has an octahedral coordination environment with N_2O_2 donor atoms of the equatorial tetradentate ligand 4-MeOhapen and N_2 donor atoms of two imidazoles at the axial positions. The Fe–N(imine) (2.107(3), 2.092(4) Å), Fe–N(imdazole) (2.151(5), 2.184(5) Å) and Fe–O (1.877(3), 1.897(3) Å) coordination bond distances and the angle of O–Fe–O (100.5(1)°) at 296 K are consistent with the reported bond lengths for HS Fe^{III} complexes with similar Schiff-base ligands [6c,7,8]. Fig. 3(b) shows the orientations of the two imidazole rings, in which the two imidazole rings are oriented nearly along the two N–Fe–O diagonals. The saturated five-memberd chelate ring takes gausche conformation, as C9 and C10 atoms deviate by +0.14 and −0.30 Å from the mean plane defined by Fe, N1, and N2, showing a gauche conformation.

Fig. 4 shows a one-dimensional (1D) chain structure at 296 K. The anion $CF_3SO_3^-$ plays as a linker by two of three oxygen atoms of $CF_3SO_3^-$, and the two oxygen atoms O(5) and O(7) are hydrogen-bonded to two imidazole groups of two adjacent cations $[Fe^{III}(Him)_2(4\text{-MeOhapen})]^+$ to produce a one-dimensional chain structure. The cation–anion hydrogen-bond distances between an imidazole nitrogen atom and anion $CF_3SO_3^-$ are O(5)···N(4) = 2.917(8) Å and O(7)···N(6)* = 2.799(9) (* denotes the corresponding atom of the adjacent unit; $-1/2 + x$, $1/2 - y$, $1/2 + z$). There is no interchain hydrogen bonds less than 3.1 Å. Due to the chirality of the gauche conformation of the five-membered chelate ring, there are two possible species of δ- and λ-$[Fe^{III}(Him)_2(4\text{-MeOhapen})]^+$. Within a chain, adjacent cations are related by c-glide plane so that δ- and λ-$[Fe^{III}(Him)_2(4\text{-MeOhapen})]^+$ species are linked via $CF_3SO_3^-$ are in the range of 2.074(12)–2.180 ion and arranged alternately (Fig. 4).

Table 1
Crystallographic data of $[Fe^{III}(Him)_2(4\text{-MeOhapen})]CF_3SO_3$ at 296 and 150 K.

Formula	$C_{27}H_{30}N_6O_7FeF_3S$	
Formula weight	695.47	
Crystal system	monoclinic	triclinic
Space group	$C2/c$ (No.15)	$P\bar{1}$ (No. 2)
T (K)	296	150
a (Å)	20.692(1)	17.124(3)
b (Å)	17.4343(7)	18.526(3)
c (Å)	18.1663(8)	20.508(3)
α (°)	90	79.743(3)
β (°)	113.014	89.315(4)
γ (°)	90	65.348(4)
V (Å^3)	6031.9(5)	5804(2)
Z	8	8
D_{calc} (g cm^{-3})	1.539	1.592
μ (mm^{-1})	6.428	6.679
R^a, Rw^b	0.0567, 01,832	0.1462, 0.3415

[a] $R = \Sigma||F_o| - |F_c||/\Sigma|F_o|$.
[b] $Rw = [\Sigma w(|F_o^2| - |F_c^2|)^2/\Sigma w|F_o^2|^2]^{1/2}$.

Table 2
Coordination bond distances, angles, and hydrogen bond distances of $[Fe^{III}(Him)_2(4\text{-}MeOhapen)]CF_3SO_3$ at 296 and 150 K.

	296 K	150 K			
	Fe	A	B	C	D
Fe–N1	2.107(3)	1.905(14)	2.106(12)	2.114(15)	2.106(13)
Fe–N2	2.092(4)	1.905(10)	2.074(12)	2.088(10)	2.094(12)
Fe–N3	2.151(5)	1.982(10)	2.142(10)	2.169(9)	2.134(10)
Fe–N5	2.184(5)	2.002(9)	2.180(11)	2.215(9)	2.175(10)
Fe–O1	1.877(3)	1.876(8)	1.861(10)	1.915(8)	1.875(9)
Fe–O2	1.897(3)	1.885(12)	1.894(10)	1.899(12)	1.898(10)
<Fe–N>	2.134	1.949	2.126	2.147	2.127
O1–Fe–O2	100.52(11)	85.4(4)	101.1(4)	101.6(5)	100.6(4)
O1–Fe–N1	88.49(13)	93.3(5)	87.7(5)	89.2(5)	87.5(5)
O1–Fe–N3	93.73(15)	89.0(4)	91.7(4)	89.2(4)	93.4(4)
O1–Fe–N5	87.82(15)	87.9(4)	90.4(4)	90.5(4)	87.7(4)
O2–Fe–N2	89.53(11)	93.7(5)	88.6(5)	87.8(5)	89.5(5)
O2–Fe–N3	90.01(13)	90.1(5)	89.3(4)	90.4(5)	89.7(4)
O2–Fe–N5	90.25(13)	87.7(5)	89.4(5)	88.0(5)	90.6(4)
N1–Fe–N2	81.41(13)	87.7(5)	82.7(5)	81.5(5)	82.4(5)
O(5)···N(4)	2.917(8)	2.718(15)	2.808(14)	2.827(15)	2.808(14)
O(7)···N(6)*	2.799(9)	2.903(14)	2.878(14)	2.873(14)	2.891(14)

(a) *; −1/2 + *x*, 1/2 − *y*, 1/2 + *z*.
(b) Interchain hydrogen bonds at 150 K.
a···d, 2.995(11); b···c, 3.037(11); N(C)···O, 3.033(16).

3.3.2. Structure at 150 K

A crystal was cooled from room temperature to 150 K and maintained at the temperature for one day, and then the X-ray diffraction experiment was started. The complex crystallized into a triclinic space group $P\bar{1}$ with Z = 8 at 150 K, indicating that the crystal underwent a structural phase transition. The crystallographic data is added to the data at 296 K in Table 1. The unique crystallographic unit consists of four $[Fe^{III}(HIm)_2(4\text{-}MeOhapen)]^+$ cations noted as **A**, **B**, **C**, and **D** and four $CF_3SO_3^-$ anions noted as **a**, **b**, **c**, and **d**. The relevant bond distances and angles of four cations are added to the corresponding values of the cation at 296 K in Table 2, where the same atom numbering system is applied to all cations and anions. Similar to the 1D structure at 296 K, the complex at 150 K has a similar one dimensional structure, in which four cations are arrayed as the repeating unit $(\textbf{–Aa–Bb–Cc–Dd–})_\infty$. Based on the Fe–N and Fe–O bond distances and O–Fe–O bond angles, the spin states of four cations are easily assigned to LS–HS–HS–HS for **A**–**B**–**C**–**D**. The Fe–N and Fe–O bond distances **B**, **C** and **D** are in the range of 2.074(12)–2.180(11), 2.088(10)–2.215(9), and 2.094(12)–2.175(10), respectively, and the O–Fe–O bond angles are around 100°. These values are close to the values at 296 K and are in the expected range for HS Fe^{III} complexes. Thus the Fe^{III} centers of **B**, **C** and **D** are in the HS state. The corresponding values of cation **A** are in the range of 1.905(10)–2.002(9) and 85.4(4)°, indicating that the cation **A** is in the LS state. The X-ray analysis confirmed an ordered [HS–HS–HS–LS] phase at 150 K. The single HS state at 296 K was converted to a symmetry-breaking [HS–HS–HS–LS] state at 150 K, accompanying a crystallographic phase transition from monoclinic *C*2/c to triclinic $P\bar{1}$. Though both at 296 and 150 K, the complex has a similar 1D structure bridged by $CF_3SO_3^-$ ion, a significant difference is found in the sequence of the gauche conformation of saturated five-membered chelate ring. While δ- and λ-$[Fe^{III}(Him)_2(4\text{-}MeOhapen)]^+$ species along the chain are arrayed alternately at 296 K, the gauche conformations at 150 K are $[\lambda, \lambda, \lambda, \delta]_{1\infty}$ or its symmetry related $[\delta, \delta, \delta, \lambda]_{1\infty}$ for $[HS(\textbf{D})–HS(\textbf{C})–HS(\textbf{B})–LS(\textbf{A})]_{1\infty}$ (Fig. 5). During the spin transition from 4HS (described as $[HS(\textbf{D})–HS(\textbf{C})–HS(\textbf{B})–HS(\textbf{A})]_{1\infty}$) to 3HS + 1LS ($[HS(\textbf{D})–HS(\textbf{C})–HS(\textbf{B})–LS(\textbf{A})]_{1\infty}$), the conformations of the five membered chelate rings change from [λ(**D**), δ(**C**), λ(B)δ(A)] at 296 K to [λ(**D**), λ(**C**), λ(B), δ(A)] at 150 K, in which the conformation of **C** changes from δ to λ, in addition to the spin state change of **A** from HS to LS. Owing to the conformation change of **C** and the spin change of **A**, hydrogen bonding manner from $CF_3SO_3^-$ ion **c** is significantly affected, as shown in Fig. 6. At 296 K, there is no interchain hydrogen bonds. On the other hand, as seen in Fig. 6, at 150 K inerchain contacts have been found between **c** and **b** and between **a** and **d**. Further interchain hydrogen bonds between **c** and

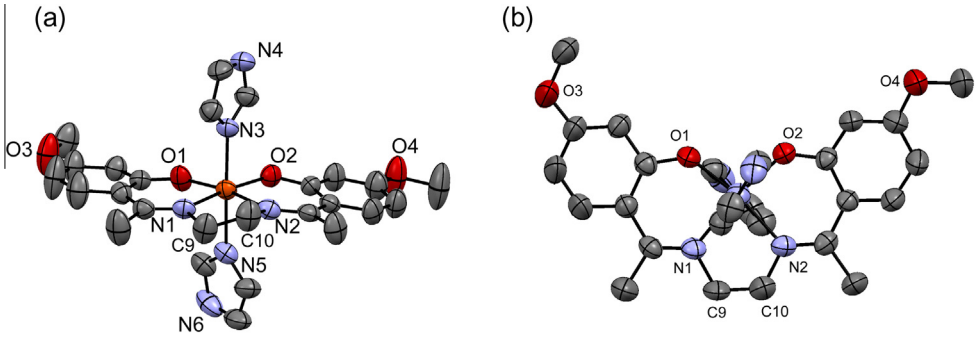

Fig. 3. (a) ORTEP drawing of $[Fe^{III}(Him)_2(4\text{-}MeOhapen)]^+$ with the atom numbering scheme at 296 K. (b) View of the complex-cation projected on the planar tetradentate ligand, showing the orientations of two imidazole rings and two methoxy groups.

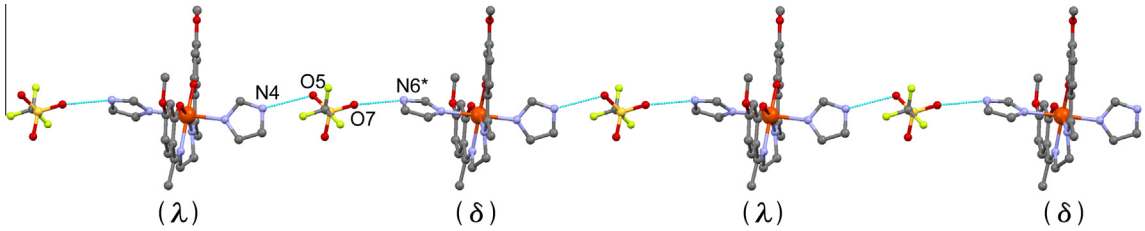

Fig. 4. 1D chain structure bridged by $CF_3SO_3^-$ of $[Fe^{III}(Him)_2(4\text{-}MeOhapen)]CF_3SO_3$ at 296 K. The chain runs along the *b*-axis and within a chain δ- and λ-species are alternately arrayed.

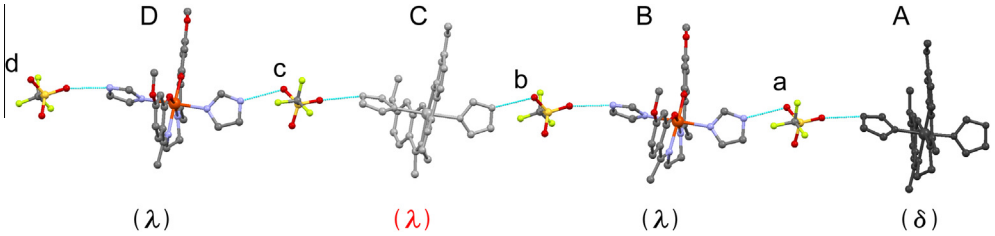

Fig. 5. 1D chain structure bridged by $CF_3SO_3^-$ of $[Fe^{III}(Him)_2(4\text{-}MeOhapen)]CF_3SO_3$ at 150 K. The crystallographic unique unit of four $[Fe^{III}(HIm)_2(4\text{-}MeOhapen)]^+$ cations (**A**, **B**, **C**, and **D**) and four $CF_3SO_3^-$ anions (**a**, **b**, **c**, and **d**). Their saturated five membered chelate rings take δ, λ, δ, λ conformations for **A**, **B**, **C**, and **D**.

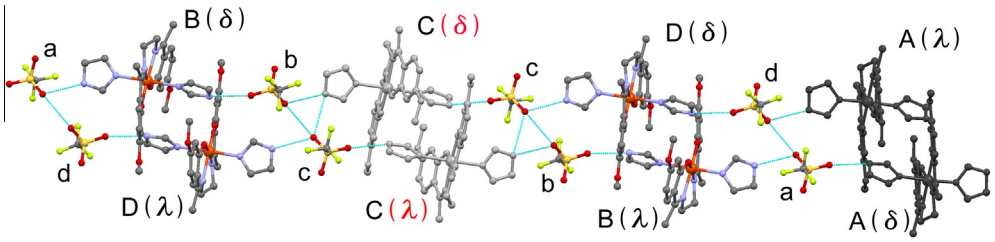

Fig. 6. Stacking manner of adjacent 1D chains and the interchain interaction through $CF_3SO_3^-$ ions. Interchain contact via. $CF_3SO_3^-$ ion is not found in the HS phase at 296 K, but $CF_3SO_3^-$ ions show inter-chain contact at 150 K.

imidazole is found, in which the imidazole forms bifurcated hydrogen bonds [15]. It can be described that this unusual [HS–HS–HS–LS] phase is stabilized by the structural change of the coordination environment and the combination of δ- and λ-conformation, and interchain interaction via $CF_3SO_3^-$. Symmetry breaking-phase transition has been observed for several compounds [10].

The CF_3SO_3 and PF_6 salts at the HS states have an isomorphous structure and showed a similar one-dimensional structure constructed by hydrogen-bonds between the anion and axial imidazole [8b]. The 1D structure should be related to abrupt and multi-step SCO properties. These two anions have a C_3 symmetry at the bridging moiety and can give one-dimensional structure. Within a one-dimensional chain, the adjacent SCO sites are well separated and the structural change (bond distance and coordination geometry) due to the spin transition can be transmitted along the chain. The CF_3SO_3 salt exhibit an abrupt spin transition between a single HS phase and a symmetry-breaking [HS–HS–HS–LS] phase and another spin transition around 80 K. On the other hand, the PF_6 salt shows an abrupt one-step spin transition. The abruptness should be brought from the hydrogen-bonded 1D structure. Interchain interaction through anion gives another cooperative effect on the SCO properties.

4. Concluding remarks

An iron(III) complex $[Fe^{III}(Him)_2(4MeOhapen)]CF_3SO_3$ was synthesized. The adjacent $[Fe^{III}(Him)_2(4MeOhapen)]$+ cations are bridged by a $CF_3SO_3^-$ ion through NH···O hydrogen bond between Him and $CF_3SO_3^-$ to give a one-dimensional chain structure $\{[Fe^{III}(Him)_2(4MeO\text{-}hapen)]CF_3SO_3\}_{1\infty}$. The complex exhibits an aburupt spin transition between the single HS state and a symmetry-breaking [HS–HS–HS–LS] state, accompanying a crystallographic phase transition from monoclinic *C*2/c at 296 K to triclinic, $P\bar{1}$ at 150 K. The unequal population of the HS and LS states of [HS(**D**)–HS(**C**)–HS(**B**)–LS(**A**)] is the result of molecular shrinkage and geometrical change of **A**, the conformational change of the saturated five-membered chelate ring of **C**, and a rearrangement of hydrogen bond network within a framework of one-dimensional structure. The magnetic susceptibility indicates another spin-transition from [HS–HS–HS–LS] to an unidentified state around 80 K. The present result suggests that multi-step spin transition with all the spin states can be observed for this type of one-dimensional complexes.

Acknowledgments

T. Fujinami was supported by the Research Fellowship for Young Scientists of the Japan Society for the Promotion of Science, KAKENHI 00248556.

Appendix A. Supplementary material

CCDC 1407204 and 1407205 contains the supplementary crystallographic data for $[Fe^{III}(Him)_2(4\text{-}MeOhapen)]CF_3SO_3$ at 296 and 150 K. These data can be obtained free of charge from The Cambridge Crystallographic Data Centre via www.ccdc.cam.ac.uk/data_request/cif. Supplementary data associated with this article can be found, in the online version, at http://dx.doi.org/10.1016/j.ica.2015.09.031.

References

[1] (a) P. Gütlich, H.A. Goodwin, Spin Crossover in Transition Metal Compounds I-III, Topics in Current Chemistry, 233–235, Springer, New York, 2004;
(b) J.A. Real, A.B. Gaspar, V. Niel, M.C. Muñoz, Dalton Trans. (2005) 2062.
[2] (a) A.H. Ewald, R.L. Martin, I.G. Ross, A.H. White, Proc. R. Soc. A280 (1984) 235;
(b) G. Harris, Theoret. Chim. Acta 5 (1966) 379;
(c) M. Zerner, M. Gouterman, H. Kobayashi, Theor. Chim. Acta 6 (1966) 363.
[3] (a) J.P. Collman, T.N. Sorrell, K.O. Hodgson, A.K. Kulshrestha, C.E. Strouse, J. Am. Chem. Soc. 99 (1977) 5180;
(b) J.P. Collman, X. Zhang, K. Wong, J.I. Brauman, J. Am. Chem. Soc. 116 (1994) 6245;
(c) D.H. Busch, N.W. Alcock, Chem. Rev. 94 (1994) 585;
(d) W.R. Scheidt, J. Am. Chem. Soc. 105 (1983) 2625;
(e) D.K. Geiger, Y.J. Lee, W.R. Scheidt, J. Am. Chem. Soc. 106 (1984) 6339.
[4] (a) Y. Nishida, S. Oshio, S. Kida, Chem. Lett. (1975) 79;
(b) Y. Nishida, S. Oshio, S. Kida, Bull. Chem. Soc. Jpn. 50 (1977) 119;
(c) Y. Nishida, K. Kino, S. Kida, J. Chem. Soc., Dalton Trans. (1987) 1157.
[5] (a) N. Matsumoto, K. Kimoto, A. Ohyoshi, Y. Maeda, Chem. Lett. (1984) 79;
(b) N. Matsumoto, K. Kimoto, A. Ohyoshi, Y. Maeda, Bull. Chem. Soc. Jpn. 57 (1984) 3307.

[6] (a) B.J. Kennedy, A.C. McGrath, K.S. Murray, B.W. Skelton, A.H. White, Inorg. Chem. 26 (1987) 483;
(b) T.M. Ross, S.M. Neville, D.S. Innes, D.R. Turner, B. Moubaraki, K.S. Murray, Dalton Trans. 39 (2010) 149.
[7] R. Hernandenz-Molina, A. Mederos, S. Dominguez, P. Gili, C. Ruiz-Perez, A. Castineiras, X. Solans, F. Lloret, J.A. Real, Inorg. Chem. 37 (1998) 5102.
[8] (a) M. Koike, K. Murakami, T. Fujinami, K. Nishi, N. Matsumoto, Y. Sunatsuki, Inorg. Chim. Acta 399 (2013) 185;
(b) T. Fujinami, M. Ikeda, M. Koike, N. Matsumoto, T. Oishi, Y. Sunatsuki, Inorg. Chim. Acta 432 (2015) 89.
[9] (a) T. Fujinami, M. Koike, N. Matsumoto, Y. Sunatsuki, A. Okazawa, N. Kojima, Inorg. Chem. 53 (2014) 2254;
(b) K. Hanahara, H. Ono, T. Fujinami, N. Matsumoto, Y. Sunatsuki, Inorg. Chim. Acta 429 (2015) 93.
[10] (a) M. Shatruk, H. Phan, B.A. Chrisostomo, A. Suleimenova, Coord. Chem. Rev. 289–290 (2015) 62;
(b) S. Bonnet, M.A. Siegler, J.S. Costa, G. Molná, A. Bousseksou, A.L. Spek, P. Gamez, J. Reedijk, Chem. Commun. (2008) 5619;
(c) K.D. Murnaghan, C. Carbonera, L. Toupet, M. Griffin, M.M. Dîrtu, C. Desplanches, Y. Garcia, E. Collet, J.F. Létard, G.G. Morgan, Chem. Eur. J. 20 (2014) 5613;
(d) M. Yamada, H. Hagiwara, H. Torigoe, N. Matsumoto, M. Kojima, F. Dahan, J. P. Tuchagues, N. Re, S. Iijima, Chem. Eur. J. 12 (2006) 4536;
(e) T. Sato, K. Nishi, S. Iijima, M. Kojima, N. Matsumoto, Inorg. Chem. 48 (2009) 7211;
(f) M. Griffin, S. Shakespeare, H.J. Shepherd, C.J. Harding, J.-F. Letard, C. Desplanches, A.E. Goeta, J.A.K. Howard, A.K. Powell, V. Mereacre, Y. Garcia, A.D. Naik, H. Muller-Bunz, G.G. Morgan, Angew. Chem., Int. Ed. 50 (2011) 896;
(g) N. Brefuel, E. Collet, H. Watanabe, M. Kojima, N. Matsumoto, L. Toupet, K. Tanaka, J.P. Tuchagues, Chem. Eur. J. 16 (2010) 14060;
(h) C.M. Grunert, S. Reiman, H. Spiering, J.A. Kitchen, S. Brooker, P. Gütlich, Angew. Chem., Int. Ed. 47 (2008) 2997.
[11] O. Kahn, Molecular Magnetism, VCH, Weinheim, Germany, 1993.
[12] CrystalStructure 4.0: Crystal Structure Analysis Package, Rigaku Corporation (2000–2010), Tokyo, Japan.
[13] (a) R. Kulmaczewski, J. Olguín, J.A. Kitchen, H.L.C. Feltham, G.N.L. Jameson, J.F. Tallon, S. Brooker, J. Am. Chem. Soc. 136 (2014) 878;
(b) M. Seredyuk, M.C. Munoz, M. Castro, T. Romero-Morcillo, A.B. Gaspar, J.A. Real, Chem. -Eur. J. 19 (2013) 6591;
(c) T. Fujinami, K. Nishi, D. Hamada, K. Murakami, N. Matsumoto, S. Iijima, M. Kojima, Y. Sunatsuki, Inorg. Chem. 54 (2015) 7291.
[14] P. Chakraborty, C. Enachescu, C. Walder, R. Bronisz, A. Hauser, Inorg. Chem. 51 (2012) 9714.
[15] H. Hagiwara, S. Hashimoto, N. Matsumoto, S. Iijima, Inorg. Chem. 46 (2007) 3136.